Increased thermal stability of activated N_2 adsorbed on K-promoted Ni{110}

Tao Liu, Israel Temprano and Stephen J. Jenkins
Department of Chemistry, University of Cambridge, Lensfield Road, Cambridge, CB2 1EW

Industrial synthesis of ammonia takes place at high temperatures and pressures via the *dissociative* adsorption of molecular nitrogen on a transition metal catalyst. In contrast, biological ammonia synthesis occurs under ambient conditions via the hydrogenation of *intact* molecular nitrogen at the active site of an enzyme. We hypothesise that the latter process may be mimicked within an inorganic system if the intact nitrogen molecule can be polarised, rendering it particularly susceptible to attack by hydrogen. Furthermore, by analogy with the surface chemistry of carbon monoxide at alkali-modified nickel and cobalt surfaces, we consider whether such a polarisation may be achieved by coadsorption with potassium on the same or similar transition metals. Here, we report on reflection absorption infrared spectroscopy results, interpreted with the aid of first-principles density functional calculations, which reveal both similarities and differences between the behaviour of carbon monoxide and nitrogen. Importantly, our calculations suggest that the surface-induced dipole of molecular nitrogen can indeed be enhanced by the coadsorbed alkali metal.

1. Introduction

Conversion of nitrogen from N_2 to the biologically active precursor, NH_3, is a pivotal chemical process to sustain life [1]. The challenge of this transformation is largely related to activation (weakening or dissociation) of the N≡N triple bond [2].

In the industrial Haber-Bosch (HB) process, rupture of the strong N≡N bond is achieved by the formation of strong N-Fe bonds at the Fe-based catalyst surface [3-10]. The resulting surface atomic N species (N_{ads}) is then hydrogenated to form NH_3 at high temperatures. Due to the exothermic nature of the NH_3 synthesis reaction, the high temperatures used in turn lead to high pressures needed to increase the NH_3 yields, making the whole process very energy intensive [11, 12]. As a result ammonia synthesis is reckoned to account for over 1% of the world´s energy production [13]. Being able to synthesize NH_3 under ambient conditions would therefore be both economically and environmentally beneficial.

It is well established that the energetic barrier to N_2 dissociative adsorption on a specific catalyst is inversely related to the N_{ads} stability on its surface [14, 15]. It is thus difficult to envisage a method to produce NH_3 at ambient conditions via a mechanism requiring prior dissociation of N_2. An alternative route to accomplish catalytic NH_3 synthesis under ambient conditions may be to directly hydrogenate molecularly adsorbed N_2 ($N_{2,ads}$). It has been demonstrated, for example, that dinitrogen can be hydrogenated using transition metal complexes at around room temperature [16-25] through coordination of the N_2 molecule to one or two transition metal centres.

Thus far, two types of molecular $N_{2,ads}$ states have been reported on transition metal surfaces, bonding in either end-on or side-on configurations [2]. The N-N bond of the side-on $N_{2,ads}$ has been found to be much weaker than that of the end-on species, the former being identified as the precursor state to high-temperature N_2 dissociation on a number of metal surfaces [2]. In contrast, the isoelectronic molecule, CO, in an end-on bonding configuration on Pd-based catalysts, can

indeed be directly hydrogenated to form CH_3OH, even at room temperature [26, 27]. In this case, the active CO species exhibit a redshifted C-O stretch frequency of ~300 cm^{-1} from the gas phase value (2130 cm^{-1}), suggesting that the intramolecular bond of CO need not be significantly weakened to activate the hydrogenation process. CO and N_2 resemble each other in both bond strength and length, but differ in their polarity and hence in their interactions with metal surfaces. From these considerations, we note that, *polarizing* $N_{2,ads}$ and *weakening* its intramolecular bond ought to be the keys to promoting hydrogenation.

Alkali metals are known to weaken and polarize coadsorbed CO molecules on transition metal surfaces, increasing the desorption temperature and leading to increased redshifts of the C-O stretch frequency [28]. In this work, we hence investigate the interactions of K with N_2 on Ni{110} surfaces. Temperature-programmed desorption (TPD) and reflection absorption IR spectroscopy (RAIRS) are used to reveal the K-induced effects on the thermal stability and N-N stretch frequency of coadsorbed N_2. Low-energy electron diffraction (LEED) is used to construct possible structural models for the coadsorbed N_2-K overlayer. Density functional theory (DFT) calculations were also conducted to understand in detail the interactions between K and N_2 on Ni{110} surfaces.

2. Experimental and theoretical methods

The experiments were performed in a UHV system comprising a main chamber and an attached optical cell, with a daily base pressure $\leq 1\times10^{-10}$ mbar. The main chamber (used for LEED, AES and TPD measurements) was equipped with a mass spectrometer, an electron gun, concentric hemispherical analyzer, LEED optics and an ion gun. The optical cell was extended from the main chamber and coupled to an FTIR spectrometer (Varian), where RAIR spectra were acquired. A detachable sample mount and a transfer arm allowed the sample to be transferred between the main chamber and the cell.

The Ni single crystal ($13\times8\times1$ mm^3, 99.999% purity) was purchased from MaTeck GmbH, polished within 0.1° of the {110} orientation. The crystal was heated by passing current through the directly welded Ta wires (0.25 mm) along the crystal edges, and cooled by liquid-N_2 via the sample mount. The minimum achievable crystal temperatures in the main chamber and the optical cell were 120 K and 110 K, respectively. The initial cleaning of the Ni{110} crystal involved cycles of 500 eV Ar^+ sputtering and 975 K annealing. Many intermediate O_2 (3×10^{-8} mbar) treatment cycles at crystal temperatures up to 850 K were also used and found to be helpful removing surface carbon contaminants. The cleanliness and surface order were monitored by AES, TPD, and LEED . The experimental apparatus and the cleaning procedure for the Ni{110} crystal has been described in detail elsewhere [29-32].

Potassium was evaporated at normal incidence from a commercial SAES getter source onto the crystal surface, positioned around 8 cm away, and the presence of K adsorbed on the sample was monitored by AES. Typically, the total base pressure was kept below 3×10^{-10} mbar during K evaporation. To have a better control of K coverage, we always allowed 120 s for the K flux to stabilise and evaporated K at a relatively slow rate. The expanded c(2×2) structure reported in the literature at saturation K coverage (θ_K=0.48 ML) on Ni{110} at 90 K [33] was obtained after 16 min K deposition on Ni{110} at 150 K. Assuming a linear K deposition rate up to saturation coverage, a deposition rate of 0.03 ML/min is derived; this estimate is used to calibrate the K coverage in all experiments presented in this work.

The quadrupole mass spectrometer (QMS) is shielded by a Au-plated cone that has an aperture of 6 mm in diameter. During TPD measurements, the QMS was brought close to the crystal surface (~1 mm) to give enhanced sensitivity to desorbing species from the surface. A linear heating rate of 1.5 K/s is used for all TPD measurements in this work.

Potassium-coverage-dependent nitrogen adsorption experiments were performed as follows. Potassium was evaporated on the clean Ni{110} surface at a particular coverage (as explained above). Base pressure conditions were then restored (typical waiting time 10 min). Potassium-precovered Ni{110} was then exposed to a background pressure of $N_{2(g)}$ of 20,000 L (200s at 1×10^{-4} Torr) for characterization. At the end of each individual experiment, the Ni{110} surface was subjected to cleaning cycles and its condition assessed (as explained above). A new cycle of potassium evaporation to a different coverage was then performed prior to background exposure to $N_{2(g)}$ for each individual subsequent experiment.

A typical RAIRS experiment was performed in the following way: after preparing the surface (cleaning/depositing K) in the main chamber, the crystal was transferred to a RAIRS-specific cell and cooled down to 125 K. A background spectrum was collected and then the crystal was subsequently exposed to N_2. Finally, a sample spectrum was recorded, either under N_2 pressure or after pumping out the N_2 gas. All spectra were averaged over 500 scans at 4 cm^{-1} resolution. The sample spectra, referenced against their corresponding background spectra, are presented with no further treatment in this paper.

In order to assist in the interpretation of experimental results, we have also conducted first-principles density functional calculations, using the CASTEP computer code [34]. Periodic boundary conditions were employed, consistent with a (2x2) surface unit cell, permitting coverages in multiples of 0.25 ML to be considered. Electronic wavefunctions were expanded within a plane wave basis set, up to a kinetic energy cut-off at 340 eV, and the Brillouin zone corresponding to the (2x2) cell was sampled on a Monkhorst-Pack mesh [35] of dimension 3x4x1. Electron-ion interactions were handled by ultrasoft pseudopotentials [36], while exchange and correlation were represented by the PW91 functional [37]. The surface was modelled by a slab comprising seven atomic layers, of which the top five were permitted to relax according to the calculated forces, and adsorbed species (K or N_2) were placed only on this "free" side. Following optimisation of the geometry, vibrational spectra were obtained by the method of finite displacements (i.e. systematic perturbation of the atomic geometry was used to generate a dynamical matrix whose diagonalisation yields the vibrational eigensolutions).

3. Results

Potassium-coverage-dependent RAIR spectra, were recorded after subjecting K-precovered Ni{110} at 125 K to a 20,000 L of N_2 exposure (Fig. 1). Each spectrum was acquired after re-establishing UHV conditions ($<3\times10^{-10}$ mbar). On an initially clean Ni{110} surface (θ_K=0 ML), $N_{2,ads}$ exhibits a single IR band at 2205 cm^{-1}. As potassium coverage increases, the corresponding N-N stretch frequency redshifts from 2205 to 2177 cm^{-1} at 0.11 ML, whereas the intensity of the $N_{2,ads}$ IR band decreases, disappearing altogether at around 0.14 ML of potassium. At potassium coverages beyond 0.17 ML, however, new peaks associated with the N-N stretching vibration appear at highly redshifted frequencies. At θ_K = 0.17 ML, the first new band appears at 2031 cm^{-1} with very low intensity. With increasing θ_K, (up to 0.35 ML) this feature further redshifts down to 1982 cm^{-1} and increases in intensity. A second feature also appears at 1950 cm^{-1} and equally

redshifts with increasing θ_K down to 1892 cm^{-1}, again reaching maximum intensity at around θ_K = 0.35 ML.

The relatively high intensities of IR bands detected in the spectra are indicative of large dynamic dipole moments of the N-N stretching vibrations, suggesting that N_2 is likely adsorbed with its molecular axis exhibiting a relatively high component normal to the surface. This strongly suggest the presence of an end-on $N_{2,ads}$ state on the surface. The variations in intensity of these N-N stretching vibrations at different levels of θ_K, alongside the continuity of frequency shifts, is indicative of variations in populations of $N_{2,ads}$ species on the surface, rather than changes in molecular conformation .

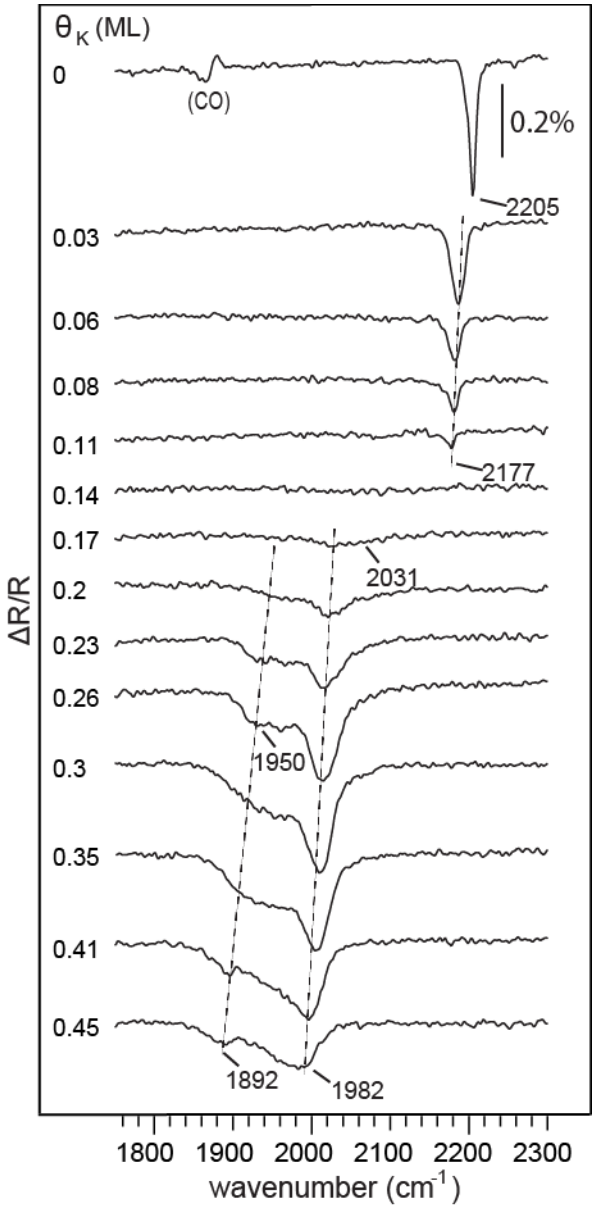

Figure 1. Potassium-coverage-dependent $^{14}N_2$ RAIR spectra recorded after exposing a K-preadsorbed Ni{110} sample at 125 K, to 20,000 L ($200\times1\times10^{-4}$ torr·s) of N_2. All RAIR spectra

were taken after evacuating the N_2 ambient pressure and re-establishing UHV conditions ($\leq 3\times10^{-10}$ mbar). Potassium was evaporated onto the sample at 300 K for all experiments, and its estimated coverage (θ_K) is noted for each spectrum.

Following the same experimental procedure TPD spectra are shown in Fig. 2. The desorption spectrum of N_2 (20,000 L) adsorbed on a clean Ni{110} surface (θ_K=0 ML) at 125 K shows a single peak at 146 K. At θ_K<0.14 ML, the single N_2 desorption peak intensity decreases with increasing potassium coverages. This is consistent with the observed reduction in the N_2 IR bands in Fig. 1 (θ_K<0.14 ML) being due to a decrease in coverage rather than a change in adsorption configuration. In addition, no clear shift is observed in the desorption temperature within the low potassium coverage range ($\leq$ 0.1ML) (Fig. 2), which indicates that the adsorption energy (assuming a non-activated adsorption state) of $N_{2,ads}$ is largely unchanged. In this range of potassium coverage, however, there is a noticeable redshift in the N-N stretching vibration frequencies of $N_{2,ads}$, (from 2205 to 2177 cm^{-1}) suggesting that the adsorption energy of $N_{2,ads}$ and its intramolecular frequency are not necessarily connected.

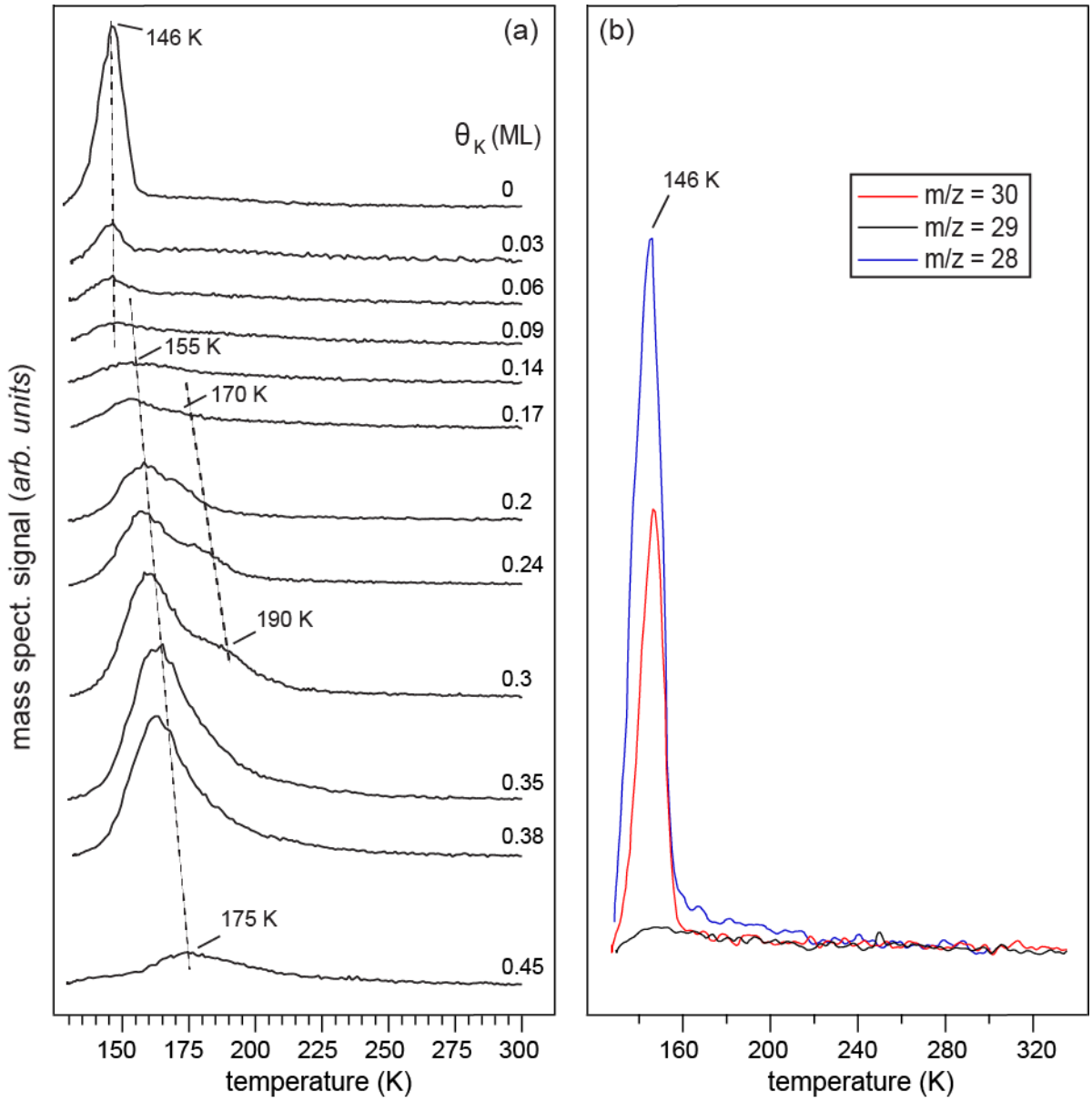

Fig. 2. (a) Potassium-coverage-dependent TPD spectra recorded after exposing a K-preadsorbed Ni{110} sample at 125 K to 20,000 L of N_2. Potassium was evaporated onto the sample at 300 K for all experiments and its estimated coverage (θ_K) is noted for each spectrum; (b) Isotopic exachange TPD where a mixture of $^{14}N_2/^{15}N_2$ was dosed at low K coverage under similar experimental conditions to (a).

Beyond 0.14 ML of potassium, new N_2 desorption peaks appear at ~160 K and ~185 K, both shifting to higher desorption temperatures with increasing potassium coverages up to θ_K=0.3 ML. In this range of potassium coverage (0.14> θ_K>0.3 ML) a higher intensity peak with a smaller shoulder is present in both the RAIRS and TPD spectra. Since the RAIR spectra seem to show a correlation between peak intensity and species population, this appears to be also the case for the

corresponding TPD spectra. To confirm this correlation, we performed temperature-dependent RAIRS measurements (Fig. 3) in the temperature range between 125 and 163 K.

Fig. 3 shows temperature-dependent RAIR spectra recorded for the adsorption of 20,000 L N_2 at 125 K on a K-preadsorbed Ni{110} surface (θ_K=0.26 ML). The spectrum labelled 125 K corresponds to the spectrum labelled θ_K=0.26 ML in Fig. 1. In the temperature range between 125 K and 142 K, a decrease in intensity of the N-N stretching vibration peak at 2004 cm^{-1} is observed, whereas the peak at 1920 cm^{-1} remains constant in intensity. The RAIR spectrum obtained at 152 K displays a single feature at 1920 cm^{-1}, which decreases in intensity upon subsequent annealing up to 163 K. From this sequence it is clear that as the temperature increases, the species producing a peak at 2004 cm^{-1} desorbs first, followed by the shoulder component (1920 cm^{-1}) at higher temperatures. The complete disappearance of the primary peak at 2004 cm^{-1} and the shoulder at 1920 cm^{-1} occur at temperatures that are broadly in agreement with the desorption peaks displayed in Fig. 2. This indicates that the $N_{2,ads}$ states observed in the range 2031-1982 cm^{-1} for potassium coverage between 0.17 ML and 0.45 ML is associated with the desorption peak at 160 K, and the $N_{2,ads}$ state observed between 1950 cm^{-1} and 1892 cm^{-1} in the same potassium coverage range is associated with the 185 K desorption peak. Furthermore, isotopic exchange TPD experiments were performed in which a potassium-preadsorbed Ni{110} surface was exposed to a mixture of $^{14}N_2/^{15}N_2$ isotopes at 125 K (Fig. 2b). These experiments showed no evidence of recombinative desorption of surface atomic N (m/z=29), revealing that the presence of K on the surface of Ni{110} does not promote N_2 dissociative adsorption. These results remarkably suggests that the more activated $N_{2,ads}$ states exhibit higher thermal stability on the surface.

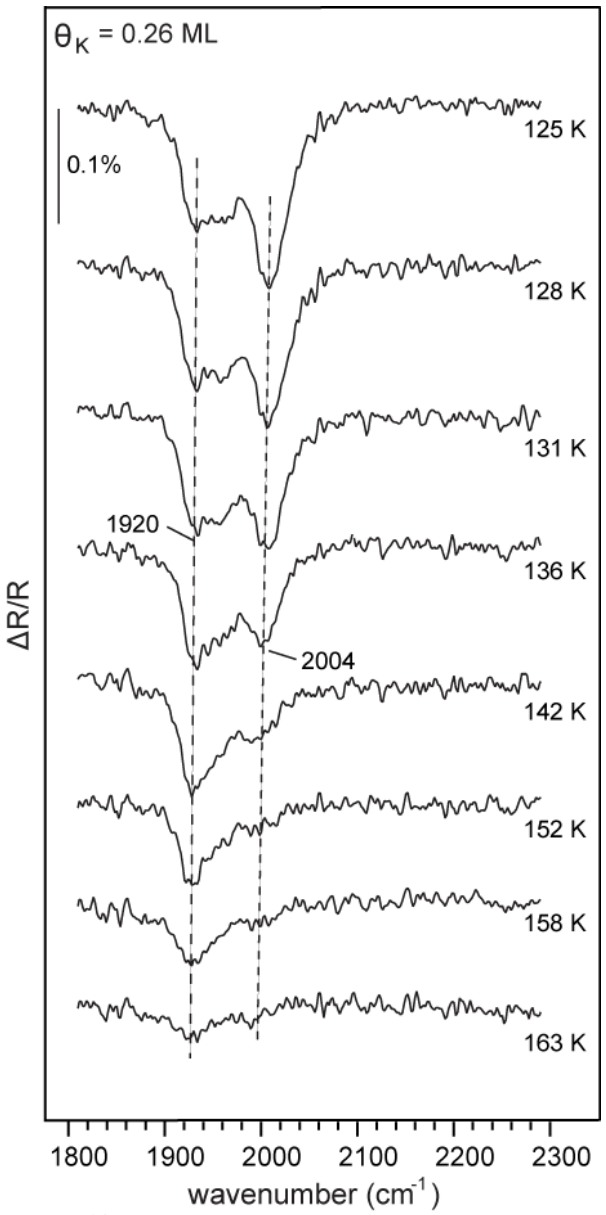

Fig. 3. Temperature-dependent $^{14}N_2$ RAIR spectra recorded on a K-preadsorbed (θ_K = 0.26 ML) Ni{110} surface exposed at 125 K to 20,000 L of N_2. The crystal temperature was raised in a stepwise manner and each spectrum was acquired at a fixed temperature indicated in the figure. Potassium was initially evaporated onto the Ni{110} surface at 300 K.

The correlation between the redshift of N-N stretching vibrations and desorption temperatures, as a function of potassium coverage, is clearly illustrated in Fig. 4. In this figure the areas of N-N stretching vibrations from Fig. 1 (in red), and total areas of desorption peaks from Fig. 2 (in black) are plotted as a function of K-coverage. Both RAIRS band intensities and TPD peak areas decrease until 0.1 ML of potassium, but then rise significantly up to 0.35 ML and subsequently drop again. This correlation reinforces the conclusion that reduction or absence of IR bands is indeed due to $N_{2,ads}$ coverage being reduced on the surface, rather than a significant conformation

change of $N_{2,ads}$. This indicates that a significantly larger amount of N_2 can be chemisorbed on Ni{110} at 125 K in the presence of potassium at $0.2 > \theta_K > 0.4$ ML.

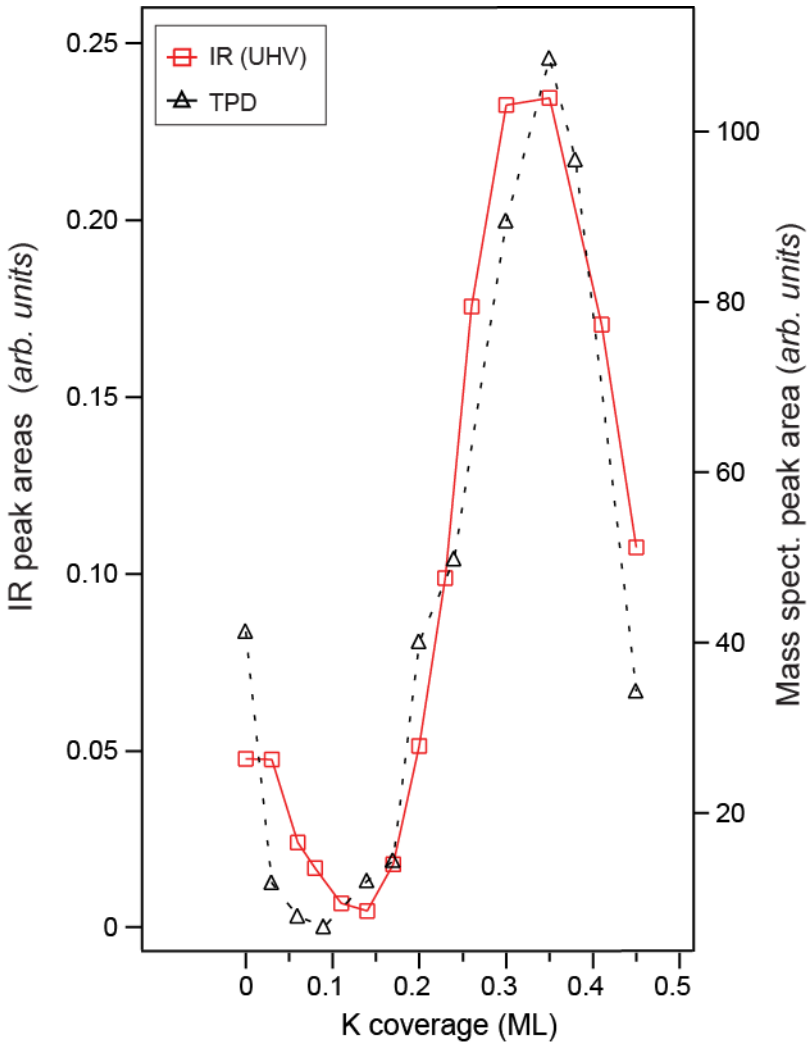

Fig. 4. N_2 RAIRS band intensities from Fig. 1 (red) and TPD peak areas from Fig. 2 (black) are plotted together to show their dependence on potassium coverage.

Fig. 5 shows LEED measurements before and after N_2 exposures on K-preadsorbed Ni{110} at 125 K; 0.25 ML and 0.35 ML K coverages were investigated, as they exhibit relatively sharp LEED pattern and have a large N_2 uptake. It is clear that for 0.25 ML K/Ni{110} (Fig. 5(a)), a single streaky beam at the (½, 0) position is seen, indicating a two-fold periodicity along the [1-10] direction. After N_2 exposure there is a general increase in brightness, indicating a nitrogen-induced surface ordering process. This results in an increase in the total ordered surface area, and thus an increase in brightness of the diffracted beams. The remaining streakiness along [001] orientation and the half order streaks at the (½, 0) position indicate that the N_2/K/Ni{110} surface superstructure possesses no periodic order along [001], but has a periodicity repeating over two Ni{110} unit meshes along [1-10] direction. A structural representation of the surface

in agreement with the LEED pattern in Fig. 5(a), and according to the above considerations, is shown in Fig. 5(b). Possible N_2 adsorption sites are labelled (a-e), in a sequence of reduced adjacent K neighbours. Based on this model, we calculated, using density functional theory, the N-N stretch frequency of $N_{2,ads}$ at each suggested site.

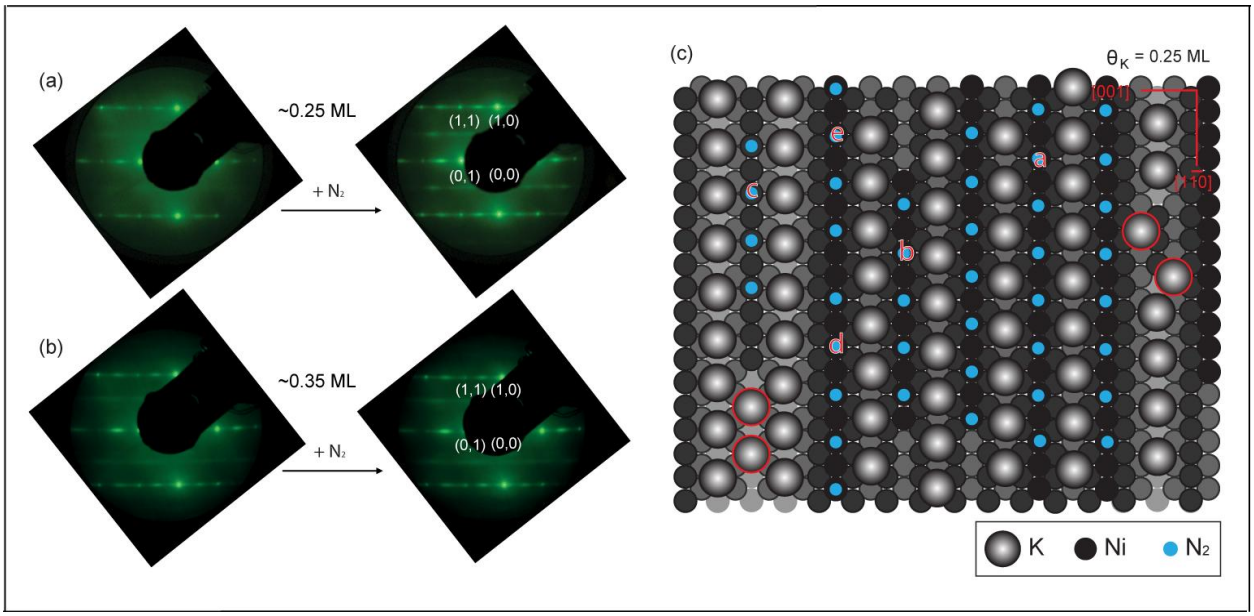

Fig. 5 LEED patterns obtained from Ni{110} at 125 K; (a) θ_K=0.25 ML and (b) θ_K=0.35 ML before and after of N_2 adsorption (20000 L at 125 K). The kinetic energy of the primary electron beam is 150 eV for all images. The surface orientation and some integer order beams are labelled in the images for clarity. (c) Structural representation of possible adsorption sites for N_2 and K in agreement with patterns present in (a).

In our DFT calculations, we initially considered the adsorption of N_2 into bridge and atop sites of the clean Ni{110} surface, at a coverage of 0.25 ML (Fig. 6). Of these, the atop site was favoured (Fig. 6a and 6b), with an adsorption energy of 0.93 eV, compared with 0.84 eV for the bridge site (Fig. 6c and 6d) (DFT typically overestimates the adsorption heat of simple diatomic molecules, but relative energies are usually meaningful). The molecule adopted an upright geometry in each case, with N-N bond lengths of 1.17 and 1.19 Å for the atop and bridge models respectively; these differing bond lengths were reflected in calculated stretch frequencies of 2221 cm^{-1} for the atop site and 2056 cm^{-1} for the bridge site. Clearly the (energetically favoured) atop site is considerably more consistent with the frequency of 2205 cm^{-1} measured in RAIRS than is the bridge site. Hirshfeld analysis indicates a net negative charge of just -0.02e on the molecule in the atop site, compared with -0.05e in the bridge site, suggesting a possible (if slight) correlation between the degree of substrate-adsorbate charge transfer and the degree of redshift observed.

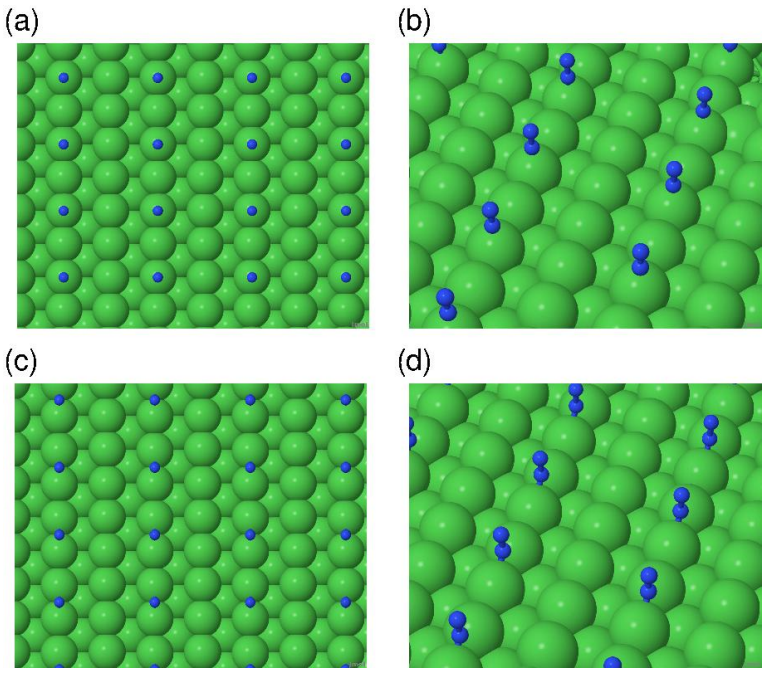

Fig. 6 Geometries resulting from DFT calculations of N_2 adsorption at 0.25 ML coverage on the clean Ni{110} surface. Panels (a) and (b) show vertical and oblique views of adsorption in the atop site of the surface's regular steps; panels (c) and (d) show the same for adsorption in the bridge site.

To model the effect of potassium coadsorption, a structural model containing 0.25 ML of the alkali metal alone on the surface (Fig. 7) was first evaluated. In this model, based upon previous LEED studies, the surface exhibits a missing-row reconstruction, with potassium atoms located in the resulting troughs. It is found that the potassium atoms acquire a net positive charge of 0.39e, thereby reducing the surface dipole moment (and hence the work function). Accordingly, it is expected that the transfer of electrons from the surface to any adsorbed N_2 molecules ought to be enhanced by the presence of coadsorbed potassium. Indeed, when considering a range of N_2 adsorption geometries on this K-preadsorbed surface this is precisely what it is observed. At a molecular coverage of 0.25 ML, there are now two distinct atop adsorption sites readily accessible on the surface, at different distances from the nearest alkali metal atom. The closer of the two atop sites turns out to be the most favoured site overall (Fig. 7(c) and (d)), with an adsorption energy of 1.16 eV. Nevertheless the furthest adsorption site from the nearest alkali atom (Fig. 7(a) and (b)) is still more favourable (adsorption energy 1.12 eV) than adsorption onto the bare surface. It follows, therefore, that the interaction between potassium and molecular nitrogen on this surface must be attractive, as one would expect when a strongly electropositive species are coadsorbed with electronegative ones. Intermediate in energy between the two atop sites is the bridge site (Fig. 7(e) and (f)), with adsorption energy 1.13 eV, while a highly tilted (31º off normal) adsorption into a three-fold hollow site is found to be metastable with adsorption energy 0.88 eV (Fig. 7(g) and (h)). The two atop sites give rise to a N-N bond length of 1.18 A (midway between the bond lengths for bridge and atop adsorption on the clean surface). The corresponding stretch frequencies of these adsorbates are only modestly redshifted, to values of 2129 cm^{-1} for the more favourable atop site and 2141 cm^{-1} for the less favourable. The bridge

site, on the other hand, accommodates a quite strongly redshifted species, with a stretch frequency of 1948 cm^{-1} (bond length of 1.20 Å) while the tilted three-fold adsorption geometry yields a stretch frequency of 1766 cm^{-1} (bond length of 1.23 Å).

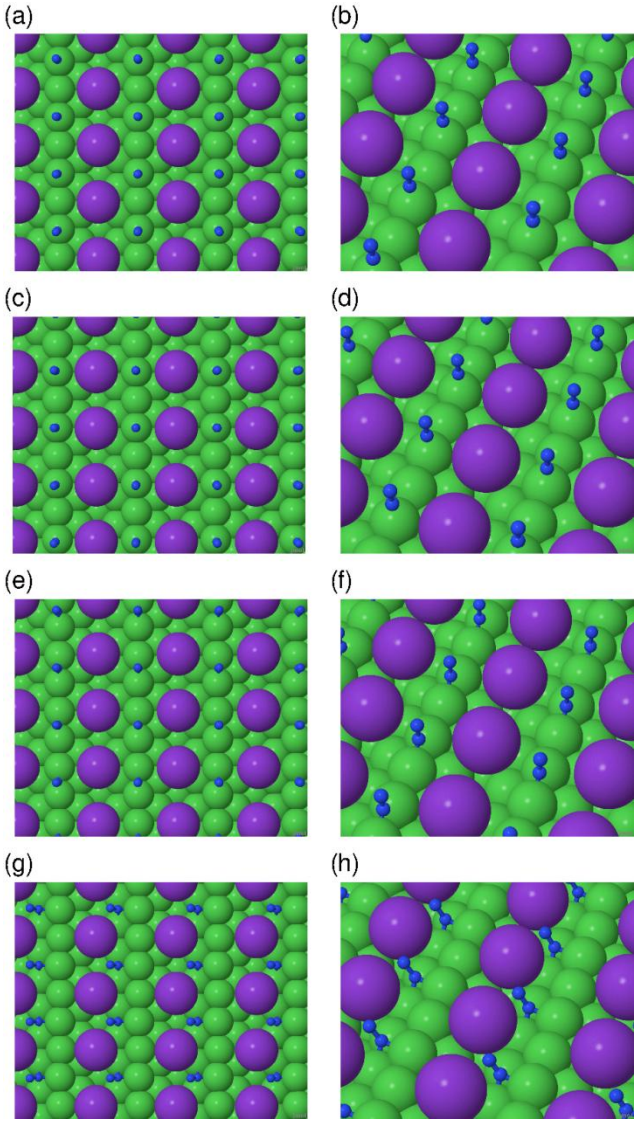

Fig. 7 Geometries resulting from DFT calculations of N_2 adsorption at 0.25 ML coverage on a Ni{110} surface pre-adsorbed with 0.25 ML atomic potassium. Panels (a) and (b) show vertical and oblique views of adsorption in the atop site most distant from the alkali metal; panels (c) and (d) show the same for adsorption in the proximal atop site. Panels (e) and (f) show top and side views of adsorption in the bridge site, while panels (g) and (h) show adsorption in a three-fold hollow site.

It is clear that these computational results do not precisely match the experimental results, since they would appear *prima facie* to indicate a preference for the weakly redshifted species even at quite high potassium coverages. We should, however, point out that the entire energy range for the three most favourable adsorption geometries considered spans less than 0.04 eV. Given the

approximations inherent in DFT, it would be most accurate to say that these calculations do not really allow us to make any definite determination of the relative stabilities of the atop and bridge sites on the basis of energetics alone. It is thus not at all unreasonable to identify the bridge site geometry with the observed absorption band at around 1940 cm^{-1} (at 0.25 ML K).

More importantly, we should also note that our assumption of a 0.25 ML N_2 coverage is, indeed, only an assumption. In fact, the increased adsorption heat calculated in the presence of K suggests that a rather higher saturation coverage might be possible at room temperature (as a very rough rule of thumb, saturation at 300 K occur at the coverage for which the adsorption heat is approximately 1 eV). Additional calculations in which 0.50 ML of N_2 was placed on the K-preadsorbed surface were therefore carried out (Fig. 8). In these, atop and bridge adsorption sites were calculated, finding adsorption heats of 1.04 eV (atop, Fig. 8(a) and (b)) and 0.99 eV (bridge, Fig. 8(c) and (d)) - both higher than the adsorption heats obtained at 0.25 ML on the clean surface. In the atop case, the calculated N-N bond lengths were 1.18 Å and 1.19 Å for the adsorbates closest and furthest from the K atom in each cell. The stretch frequencies in this model were 2081 cm^{-1} and 2148 cm^{-1} respectively, the lower relating to vibration of neighbouring molecules out of phase with one another, while the higher represents an in-phase relationship; both should be in principle detectable by RAIRS, as the weightings on each molecule are not identical, precluding cancellation of dynamic dipoles in the out-of-phase case. In the bridge case, the N-N bond length was 1.20 Å for both molecules, with the in-phase stretch frequency calculated to be 2004 cm^{-1} and the (undetectable) out-of-phase mode calculated at 1941 cm^{-1}. In this case, the out-of-phase mode may not be strictly observable in RAIRS, since the weighting on each molecule is identical, meaning that the net dynamic dipole moment should be zero. On the real surface, however, it is likely that N_2 is distributed in a disordered fashion, so whilst the present result gives a sense of the frequency of the mode, one should not read too much into the precise cancellation of the dynamic dipole moments. These results suggest that the bridge adsorption model is quite consistent with the strongly redshifted feature in RAIRS (around 1940 cm^{-1}). The atop model also fits reasonably well with the moderately redshifted feature (around 2020 cm^{-1}) observed at a K precoverage of 0.25 ML. Quite why no absorption band is observed experimentally around 2150 cm^{-1} remains to be answered, however.

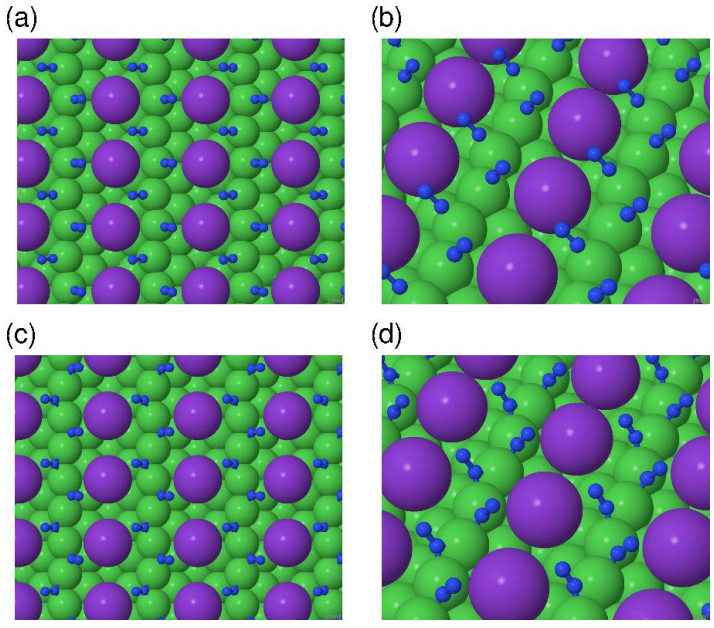

Fig. 8 Geometries resulting from DFT calculations of N_2 adsorption at 0.5 ML coverage on a Ni{110} surface pre-adsorbed with 0.25 ML atomic potassium. Panels (a) and (b) show vertical and oblique views of adsorption in atop sites; panels (c) and (d) show the same for adsorption in the bridge sites.

Comparing these results with the adsorption of N_2 in the absence of potassium, all the models considered here involve enhanced electron transfer from the surface to the molecule. At 0.25 ML N_2 coverage, the molecule gains negative charges of -0.13e and -0.12e in the more and less favoured atop sites respectively, -0.16e for the bridge site, and -0.19e for tilted adsorption in the three-fold site; the positive charge on potassium is 0.42-0.43e for all but the latter geometry, where it falls to 0.39e. At 0.50 ML N_2 coverage, the charge transfer is not quite so marked, with the molecule gaining negative charges of -0.09e and -0.08e in the atop case, with -0.10e for both molecules in the bridge case; the positive charge on potassium is 0.36e in the former situation, and 0.38e in the latter. Although the adsorption of N_2 in the current system was rationalised by charge transfers mediated via the surface, it is worth noting that direct electrostatic interactions of K^+ with N_2 may also play a role in determining the $N_{2,ads}$ stability and its intramolecular bond strength, especially at higher K coverages.

In the case of Li coadsorption with N_2 on Ni{110}[30], we have previously identified two types of N_2-Li interactions when co-adsorbing Li and N_2 on Ni{110}: (1) a continuous monotonic redshift in N-N frequency occurs from 2205 cm^{-1} on a clean Ni{110} surface to 2114 cm^{-1} on a Li-preadsorbed (0.94 ML) surface, accompanied by a reduction in $N_{2,ads}$ desorption temperatures (<146 K); (2) at the highest Li coverages (0.94 ML), another two $N_{2,ads}$ states also appear at 2050 and 1950 cm^{-1} desorbing at 160 K, although the uptake of $N_{2,ads}$ is very small. By contrast, coadsorption with K leads to larger redshifts of N-N below 1900 cm^{-1} and increased thermal stability (T_{des}=190 K) at modest K coverages, and thus a higher $N_{2,ads}$ uptake. These features associated with K are favourable toward promoting hydrogenation of molecular $N_{2,ads}$.

Turning to the question of molecular polarisation, our DFT results support the notion that N_2 is polarised when adsorbed end-on at the Ni{110} surface, with the distal end more negatively charged than the proximal. The distribution of Hirshfeld charges corresponds to a dipole moment per molecule of 0.17 D in the case of atop adsorption, with 0.14 D for adsorption in the bridge site (N.B. 1 D = 3.33564×10^{-30} Cm). In the presence of coadsorbed potassium, however, the molecular polarisation increases, falling in the range 0.26-0.31 D for the atop and bridge sites at both 0.25 ML and 0.50 ML coverages of N_2. In the highly tilted site found at 0.25 ML N_2 coverage on the potassium covered surface, the polarisation rises to 0.50 D, although energetic considerations suggest that this must be very much a minority species.

4. Conclusion

We have identified two distinct K-induced effects on N_2/Ni{110}. One type of effect dominates below 0.14 ML of atomic potassium: IR bands of $N_{2,ads}$ states redshift from 2205 to 2177 cm^{-1} with increasing potassium coverage, where little variation in the corresponding desorption temperatures is seen; this is also accompanied with a decreased N_2 uptake on the surface at 125 K. The other type of effect becomes clear beyond 0.2 ML of potassium: more strongly redshifted $N_{2,ads}$ states appear between 1850 and 2000 cm^{-1} with even higher desorption temperatures than those on clean Ni{110} surfaces; they further downshift in frequency with increasing potassium

coverage and the N_2 uptake is increased as a result of the coadsorbed potassium. First-principles density functional calculations support the notion that an attractive electrostatic interaction between potassium and N_2 is responsible for these effects, via enhanced back-donation, and indicate an approximate doubling of the surface-induced molecular dipole due to the influence of the coadsorbed alkali metal.

5. References

[1] V. Smil (Editor), Enriching the Earth, The MIT Press, Cambridge, Massachussets, 2001.
[2] D.A. King and D.P. Woodruff (Editors), The chemical physics of solid surfaces and heterogeneous catalysis, Elsevier Science Publishing Company, 1991.
[3] F. Bozso, G. Ertl, M. Grunze and M. Weiss, Journal of Catalysis, 49 (1977) 18.
[4] G. Ertl, Catalysis Reviews, 21 (1980) 201.
[5] G. Ertl and M. Huber, Journal of Catalysis, 61 (1980) 537.
[6] G. Ertl, M. Huber, S.B. Lee, Z. Paál and M. Weiss, Applications of Surface Science, 8 (1981) 373.
[7] G. Ertl and N. Thiele, Applications of Surface Science, 3 (1979) 99.
[8] F. Bozso, G. Ertl, M. Grunze and M. Weiss, Applications of Surface Science, 1 (1977) 103.
[9] M. Grunze, F. Bozso, G. Ertl and M. Weiss, Applications of Surface Science, 1 (1978) 241.
[10] F. Bozso, G. Ertl and M. Weiss, Journal of Catalysis, 50 (1977) 519.
[11] M. Bowker, in D.A. King (Editor), The Chemical Physics of Solid Surfaces, Vol. 6, Elsevier, Amsterdam, 1990, p. 225
[12] M. Bowker, I. Parker and K.C. Waugh, Surface Science, 197 (1988) L223.
[13] R. Schlögl, Angewandte Chemie International Edition, 42 (2003) 2004.
[14] J.K. Nørskov, T. Bligaard, A. Logadottir, S. Bahn, L.B. Hansen, M. Bollinger, H. Bengaard, B. Hammer, Z. Sljivancanin, M. Mavrikakis, Y. Xu, S. Dahl and C.J.H. Jacobsen, Journal of Catalysis, 209 (2002) 275.
[15] S. Dahl, A. Logadottir, C.J.H. Jacobsen and J.K. Nørskov, Applied Catalysis A: General, 222 (2001) 19.
[16] T. Shima, S. Hu, G. Luo, X. Kang, Y. Luo and Z. Hou, Science, 340 (2013) 1549.
[17] K. Arashiba, K. Sasaki, S. Kuriyama, Y. Miyake, H. Nakanishi and Y. Nishibayashi, Organometallics, 31 (2012) 2035.
[18] K. Arashiba, Y. Miyake and Y. Nishibayashi, Nat Chem, 3 (2011) 120.
[19] D. Pun, C.A. Bradley, E. Lobkovsky, I. Keresztes and P.J. Chirik, Journal of the American Chemical Society, 130 (2008) 14046.
[20] M.M. Rodriguez, E. Bill, W.W. Brennessel and P.L. Holland, Science, 334 (2011) 780.
[21] P. Avenier, M. Taoufik, A. Lesage, X. Solans-Monfort, A. Baudouin, A. de Mallmann, L. Veyre, J.-M. Basset, O. Eisenstein, L. Emsley and E.A. Quadrelli, Science, 317 (2007) 1056.
[22] J.A. Pool, E. Lobkovsky and P.J. Chirik, Nature, 427 (2004) 527.
[23] K.C. MacLeod and P.L. Holland, Nat Chem, 5 (2013) 559.
[24] J.S. Anderson, J. Rittle and J.C. Peters, Nature, 501 (2013) 84.
[25] J. Murakami and W. Yamaguchi, Scientific Reports, 2 (2012) 407.
[26] Y. Kikuzono, S. Kagami, S. Naito, T. Onishi and K. Tamaru, Faraday Discussions of the Chemical Society, 72 (1981) 135.
[27] A. Palazov, G. Kadinov, C. Bonev and D. Shopov, Journal of Catalysis, 74 (1982) 44.
[28] S.J. Jenkins and D.A. King, Journal of the American Chemical Society, 122 (2000) 10610.

[29] T. Liu, I. Temprano, S.J. Jenkins, D.A. King and S.M. Driver, Physical Chemistry Chemical Physics, 14 (2012) 11491.
[30] T. Liu, I. Temprano, S.J. Jenkins and D.A. King, The Journal of Chemical Physics, 139 (2013) 184708.
[31] T. Liu, I. Temprano, S.J. Jenkins, D.A. King and S.M. Driver, The Journal of Physical Chemistry C, 117 (2013) 10990.
[32] T. Liu, I. Temprano, D.A. King, S.M. Driver and S.J. Jenkins, Chemical Communications, 51 (2015) 537.
[33] R.J. Behm, D.K. Flynn, K.D. Jamison, G. Ertl and P.A. Thiel, Physical Review B, 36 (1987) 9267.
[34] S.J. Clark, M.D. Segall, C.J. Pickard, P.J. Hasnip, M.J. Probert, K. Refson and M.C. Payne, Z. Krystallogr., 220 (2005) 567.
[35] H.J. Monkhorst and J.D. Pack, Phys. Rev. B, 13 (1976) 5188.
[36] D. Vanderbilt, Phys. Rev. B, 41 (1990) 7892.
[37] J.P. Perdew, J.A. Chevary, S.H. Vosko, K.A. Jackson, M.R. Pederson, D.J. Singh and C. Fiolhais, Phys. Rev. B, 46 (1992) 6671.